

ASTRONOMICAL DATING AND MODELING OF THE LAST 200,000 YEARS

André BERGER¹

ABSTRACT. A few experiments have been made to test the response of the Louvain-la-Neuve two-dimension northern hemisphere climate model (here named LLN 2-D model) to both the insolation and CO₂ forcings. The daily insolation values are calculated from Berger (1978). For the past 200 kyr, the atmospheric CO₂ concentration reconstructed by Jouzel *et al.* (1993) from the Vostok ice core is used. Results of these experiments show that the forcing by insolation only is able to generate, through feedbacks, long-term variations of the northern hemisphere ice volume which parallel the geological records. Moreover, the LLN 2-D model forced by both the insolation and the Jouzel CO₂ reconstruction is simulating a long-term variation of the northern hemisphere ice volume which fits the SPECMAP isotope record reasonably well, being given the limits imposed by the assumptions made for building and running this model.

KEYWORDS: Global Change, climate model, insolation, CO₂ forcing

1. ASTRONOMICAL THEORY OF PALEOCLIMATES

The incoming solar radiation received over the Earth has an annual periodic variation due to the Earth's elliptic translation motion around the Sun. In addition, the seasonal and latitudinal distributions of this solar radiation have a long-period variation due to the so-called long-term variations in the orbital elements. These are the eccentricity, e , a measure of the shape of the Earth's orbit around the Sun, the obliquity, ε , the tilt of the equator with respect to the plane of the Earth's orbit, and the climatic precession, $e \sin \varpi$, a measure of the Earth-Sun distance at the summer solstice (ϖ being the longitude of the perihelion measured from the moving equinox; seasons referred to in this paper are always specific to the northern hemisphere). Their long-term variations over the last few million years can be expressed in trigonometrical form as quasi-periodic functions of time:

$$\begin{aligned} e \sin \varpi &= \sum P_i \sin(\alpha_i t + \eta_i) \\ \varepsilon &= \varepsilon^* + \sum A_i \cos(\gamma_i t + \zeta_i) \\ e &= e^* + \sum E_i \cos(\lambda_i t + \phi_i) \end{aligned}$$

where the amplitudes P_i , A_i , E_i , the frequencies α_i , γ_i , λ_i and phases η_i , ζ_i , ϕ_i are given in Berger (1978) for calculations over one million years. Berger and Loutre (1991) and Laskar *et al.* (1993) have calculated similar long-term variations to be used for longer periods of times.

Over the past 3×10^6 years, the eccentricity of the Earth's orbit varies between near circularity ($e = 0$) and slight ellipticity ($e = 0.07$) at a period whose mean is about 100 kyr. The most important terms in the series expansion occur however at 404, 95, 124, 99, 131 and 2380 kyr (in decreasing order of the amplitudes). The tilt of the Earth's axis varies between about 22° and 25° at a period of nearly 41 kyr. Although this period corresponds to the amplitude which is by far the largest in the series expansion, there are two other important terms with periods of 54 and 29 kyr. As far as precession is concerned, two components must be considered. The first one is the axial precession in which the torque of the Sun, the Moon and the planets on the Earth's equatorial bulge causes the axis of rotation to wobble like that of a spinning top. The net effect is that the North Pole describes clockwise a circle in space (provided the mutations, i.e. terms with small amplitude and much smaller periods, are neglected) with a period of $\sim 25,800$ years correspond-

¹ Université catholique de Louvain, Institut d'Astronomie et de Géophysique G. Lemaître, Chemin du Cyclotron 2 - B-1348 Louvain-la-Neuve, Belgium.

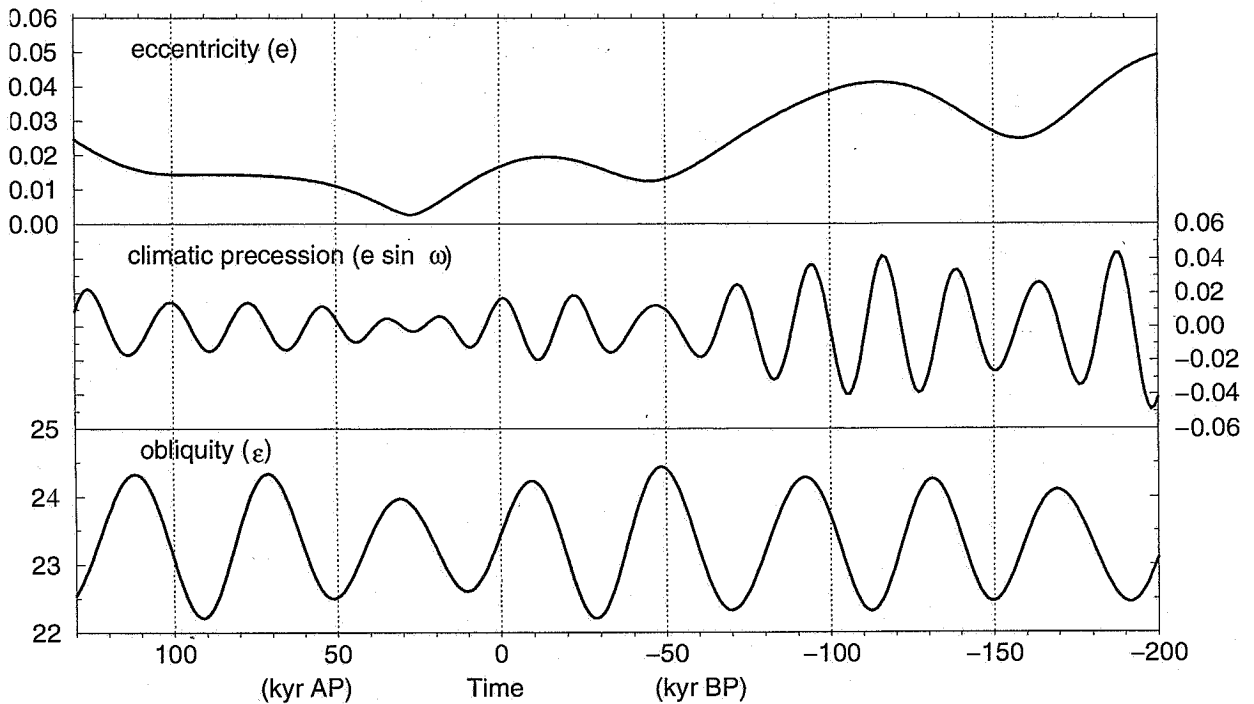


Figure 1. Long-term variations of the astronomical parameters (eccentricity, climatic precession and obliquity) over the last 200 kyr and the next 130 kyr (Berger, 1978).

ing to the period of the vernal equinox against a fixed reference point. The second is related to the fact that the elliptical figure of the Earth's orbit is itself rotating counterclockwise in the same plane leading to an absolute motion of the perihelion whose period, measured relative to the fixed stars, is about 100 kyr (the same as for the eccentricity). The two effects together result in what is known as the climatic precession of the equinoxes, a motion mathematically described by ω and in which the equinoxes and solstices shift slowly around the Earth's orbit relative to the perihelion, with a mean period of 21 kyr. This period results actually from the existence of two periods which are close to each other: 23 and 19 kyr. In the insolation formulas used to study past and future astronomical forcing of climate, the amplitude of $\sin\omega$ is modulated by eccentricity in the term $e\sin\omega$.

Because of this climatic precession, while today the winter solstice occurs near perihelion ($e\sin\omega = 0.016$, Figure 1), during the Late Glacial, roughly 10 kyr BP, it occurred near aphelion ($e\sin\omega = -0.018$, Figure 1). Moreover, because the lengths of the seasons vary in time according to Kepler's second law, the solstices and equinoxes occurred at different calendar dates during the geological past and will alter in the future (Berger and Loutre, 1994). Presently in the northern hemisphere, the longest seasons are spring (92d 19h) and summer (93d 15h), while fall with 89d 20h and winter (89d) are notably shorter. In ~ 1250 AD spring

and summer had the same length (as did fall and winter) because the winter solstice was occurring at the perihelion. About 4500 years into the future, the northern hemisphere spring and winter will have the same shorter length and consequently summer and fall will be equally long.

The combined influence of changes in e , Σ , and $e\sin\omega$ produces a complex pattern of insolation variations. A detailed analysis of the changes in solar radiation (Berger *et al.*, 1993) shows that it is principally affected by variations in precession, although the obliquity plays an important role for high latitudes, mainly in the winter hemisphere. Changes in incoming solar radiation due to changes in tilt are the same in both hemispheres during the same local season: an increase of ϵ , leads to an increase of insolation in the summer hemisphere and a decrease in the winter hemisphere. The precession effect can cause warm winters and cool summers in one hemisphere while causing the opposite effects in the other hemisphere. For example, portions of the northern hemisphere receive during present winter as much as 10 % more insolation than 11 kyr BP when the perihelion occurred in the northern hemisphere summer.

The orbital hypothesis of climatic change was first quantitatively formulated by the astronomer Milutin Milankovitch in the 1920s (Berger, 1988; Milankovitch, 1995). He argued (Milankovitch, 1941) that

insolation changes in the high northern latitudes during the summer season were critical to the formation of continental ice sheets. During periods when insolation in the summer was reduced, the snow of the previous winter would tend to be preserved - a tendency that would be enhanced by the high albedo of the snow and ice areas. Eventually, the effect of this positive feedback would lead to the formation of persistent ice sheets.

A simple linear version of the Milankovitch model would therefore predict that the total ice volume and climate over the Earth would vary with the same regular pattern as the insolation; this means that the proxy record of climate variations would contain the frequencies of the astronomical parameters that are responsible for changing the seasonal and latitudinal distributions of the incoming solar radiation. It happens that investigations during the last twenty years have indeed demonstrated that the 19 kyr, 23 kyr and 41 kyr periodicities actually occur in long records of the Quaternary climate (Hays *et al.*, 1976). The geological observation of the bipartition of the precessional peak, confirmed in astronomical computations by Berger (1977), was one of the first most delicate and impressive tests of the Milankovitch theory. However, the same investigation identified also the largest climatic cycle as being 100 kyr. As this eccentricity cycle is very weak in the insolation (Berger *et al.*, 1993a), it cannot be related to the orbital forcing by any simple linear mechanism.

2. LLN 2-D MODEL

It was suggested earlier (Berger, 1976 and 1979) that the time-evolution of the latitudinal distribution of the seasonal pattern of insolation is the key factor driving the behaviour of the climate system while the complex interactions between its different parts amplify this orbital perturbation. That dynamical behaviour of the seasonal cycle suggests that time-dependent coupled climate models might be able to test whether or not the astronomical forcing can drive the long-term climatic variations. Such time-dependent climate models must therefore be forced only by the astronomical variations of insolation for each latitude and day, the so-called boundary conditions used in equilibrium atmospheric general circulation model experiments (ice-sheet size and area, sea-surface temperature, albedo ...) being all generated by the climate model itself.

Such a climate model (designated by LLN, Louvain-la-Neuve) which links the northern hemisphere atmosphere, ocean mixed layer, sea-ice, ice sheets and continents, has been validated for the present-day climate

(Gallée *et al.*, 1991). It is a latitude-altitude model. In each latitudinal belt, the surface is divided into at most seven oceanic or continental surface types, each of which interacting separately with the subsurface and the atmosphere. The oceanic surfaces are ice-free ocean and sea-ice cover, while the continental surfaces are the snow-covered and snow-free lands and the northern hemisphere ice sheets. The atmospheric dynamics is represented by a zonally averaged quasi-geostrophic model, which includes a new parameterization of the meridional transport of quasi-geostrophic potential vorticity and a parameterization of the Hadley sensible heat transport. The atmosphere interacts with the other components of the climate system through vertical fluxes of momentum, heat and water vapour. The model explicitly incorporates detailed radiative transfer, surface energy balances, and snow and sea-ice budgets. The vertical profile of the upper ocean temperature is computed by a mixed-layer model which takes into account the meridional convergence of heat. Sea ice is represented by a thermodynamic model including leads and a new parameterization of lateral accretion. Simulation of the present climate shows that the model is able to reproduce the main characteristics of the general circulation (Gallée *et al.*, 1991). The seasonal cycles of oceanic mixed layer, sea ice, and snow cover are also pretty well reproduced.

The atmosphere-ocean model is asynchronously coupled to a model of the three main northern hemisphere ice sheets and their underlying bedrock in order to assess the influence of several factors (processes and feedbacks), including snow-surface albedo over the ice sheets, upon ice-age simulations using astronomically-derived insolation and CO₂ data from the Vostok ice core as forcings (Berger *et al.*, 1990; Gallée *et al.*, 1992).

As the model does not contain any carbon cycle, the CO₂ concentration is also considered as an external forcing. Experiments were first conducted over the last glacial-interglacial cycle for which excellent data are available. Simulation over the last two glacial-interglacial cycles were only possible when the CO₂ concentration became available for the last 200 kyr (Gallée *et al.*, 1993). In all simulations, a particular emphasis was put on the continental ice volume changes because it is a parameter of global character and one of the most widely known. Sensitivity experiments to different CO₂ concentrations (geological reconstructions as well as constant values) are expected to allow us to estimate the importance of its changes in explaining the ice volume changes through geological times. Possible thresholds for the building and the melting of the ice-sheets will be tentatively identified.

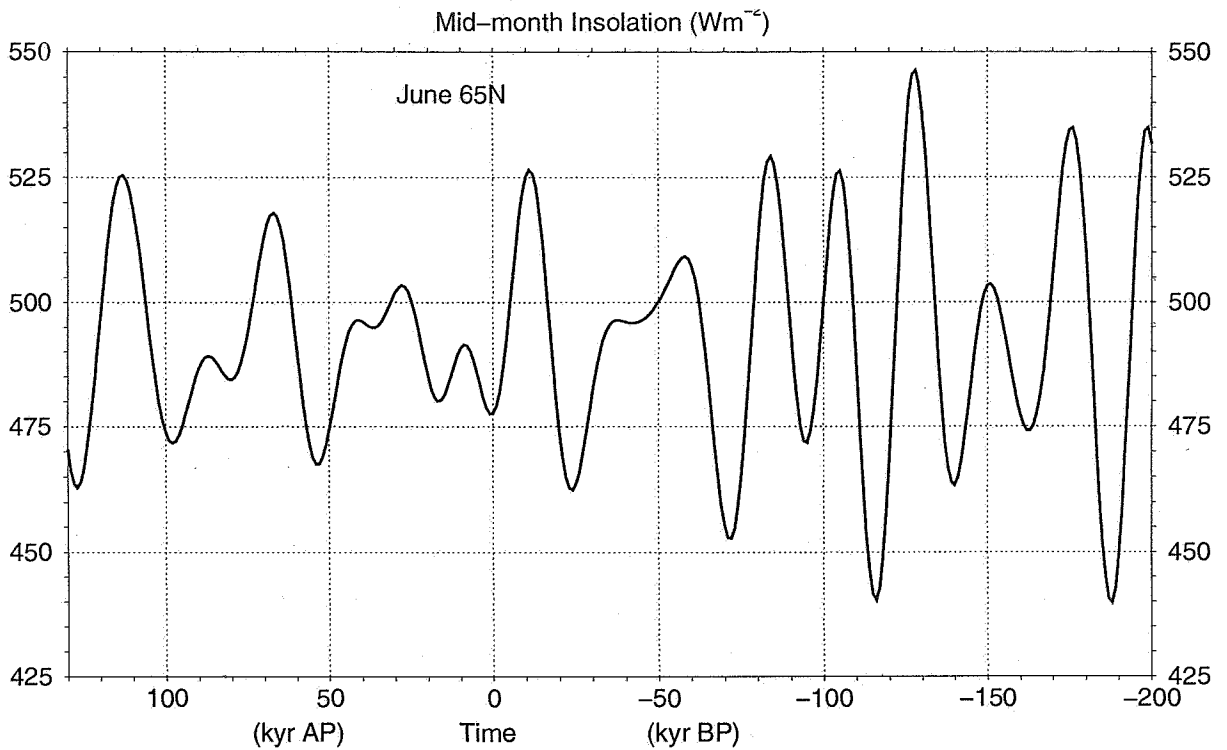


Figure 2. June mid-month insolation at 65°N over the last 200 kyr and the next 130 kyr (Berger, 1978).

3. INSOLATION FORCING OVER THE LAST 220 KYR

June insolation at 65°N (Figure 2) is very often used as a guideline for the analysis of climatic changes and, in particular, for ice volume changes. According to the Milankovitch theory (1941), these latitude and time are indeed the most sensitive ones for explaining the ice-sheets waxing and waning. Experiments made with the 2-D LLN model (Gallée *et al.*, 1992) have also shown that the ice-sheet changes are mainly driven by the ice ablation which is directly related to the summer insolation. Moreover, using this particular latitude does not bias the conclusions because for a given month, the insolation changes are in phase for all latitudes, except those which are close to the polar night (where the energy received from the Sun is very weak). Actually, the insolation changes are in phase for all latitudes where precession dominates (Berger *et al.*, 1993).

As we are primarily interested by the climate response of the LLN 2-D model over the last and next glacial-interglacial cycles, let us first concentrate upon the insolation behaviour from 220 kyr BP to 130 kyr AP. The 65°N June irradiation is maximum around 220 kyr BP (~ 550 Wm⁻²), then decreases to ~ 460 Wm⁻² over the next 10,000 years and increases again up to 535 Wm⁻² at 199 kyr BP. At 215 kyr BP the value is 516

Wm⁻²; this is the date of isotopic event 7.3, it means the interglacial peak of isotopic stage 7 in the stack oxygen-isotope record of SPECMAP (Martinson *et al.*, 1987). It is important to note that from 244 to 190 kyr BP, i.e. during the whole isotopic stage 7, the amplitude of the insolation variations is maximum, reaching more than 20% per 10,000 years, in particular at 65°N in June, a record over the last one million years. This is due to the maximum value of the eccentricity peaking at about 0.05 and a maximum variation of obliquity (Figure 1). Between 232 and 231 kyr BP, the obliquity reaches a minimum value of 22°, eccentricity is equal to 0.042 and summer solstice occurs at aphelion, which leads to an absolute minimum insolation of 434 Wm⁻² at 65° in June. Twelve thousands years later (at 219 kyr BP), $e = 0.048$, $\epsilon \sim 24^\circ$ and summer solstice is at perihelion leading to a maximum of insolation of 550 Wm⁻² in June at 65°N, a record which occurs only three times over the last million years at 579, 219 and 128 kyr BP.

A quick look to this 65°N June insolation over the last two glacial-interglacial cycles (Figure 2) shows easily that from 220 kyr BP to 70 kyr BP (~ isotopic event 4.23), this insolation (and also the insolation of the other months and latitudes) is characterized by large variations, except from 165 to 135 kyr BP (Berger, 1978; Berger and Loutre, 1991). Over the last glacial-interglacial cycle, the 65°N insolation starts to decrease

at 133, 128 and 122 kyr BP for March, June and September respectively. Summer insolation therefore peaks around 125 kyr BP in high northern latitudes. The following minimum is reached 11 to 12 kyr later. For June, insolation decreases of almost 20 % from 546 Wm^{-2} to 440 Wm^{-2} . These latitudes and months are characterized by a strong precession signal whereas, in December, obliquity dominates the spectrum at this latitude close to the polar night (Berger *et al.*, 1993), the 65°N December insolation maxima and minima occurring alternatively at 147, 130, 115 and 89 kyr BP. From 140 to 70 kyr BP (it means about during the whole isotopic stage 5), the insolation variations are almost as large as during isotopic stage 7. The seasonal and latitudinal changes in solar radiation caused by orbital changes are approximately twice as large at 125 kyr BP as at 9 to 6 kyr BP. This is because the eccentricity of the Earth's orbit was significantly larger than (0.04), so that the Earth-Sun distance was significantly smaller at perihelion (by 3 %), and because perihelion passage occurred in northern summer around 125 kyr BP, whereas it occurs now in northern winter. In the northern hemisphere high latitudes, summer radiation was increased by more than 50 Wm^{-2} (12-13 %) compared to present, winter radiation was slightly decreased and the annual average insolation was increased by 3 to 4 Wm^{-2} .

After 70 kyr BP, the amplitude of the insolation variations become smaller and between 60 and 34 kyr BP, the 65°N June insolation does even not change very much. It is also a time when the precessional period almost disappears creating a long cycle between the two minima of 70 and 20 kyr BP. A more or less similar behaviour will happen between 17 and 55 kyr AP.

4. RESPONSE OF THE LLN MODEL TO THE INSOLATION AND CO_2 FORCINGS

As the CO_2 concentration has varied in the past, it is important to see how the response of the LLN 2-D model to the orbitally induced forcing alone is modified by using the reconstructed variable CO_2 as an additional forcing.

The strongest signal found in proxy records of the ice volume being related to a 100-kyr periodicity (Imbrie *et al.*, 1993), the astronomical theory has to be tested over a period of time allowing to see whether this period can be correctly simulated. This is why the last two glacial - interglacial cycles seems to be an appropriate choice. In addition, it is also the largest multiple of 100 kyr for which two CO_2 reconstructions are

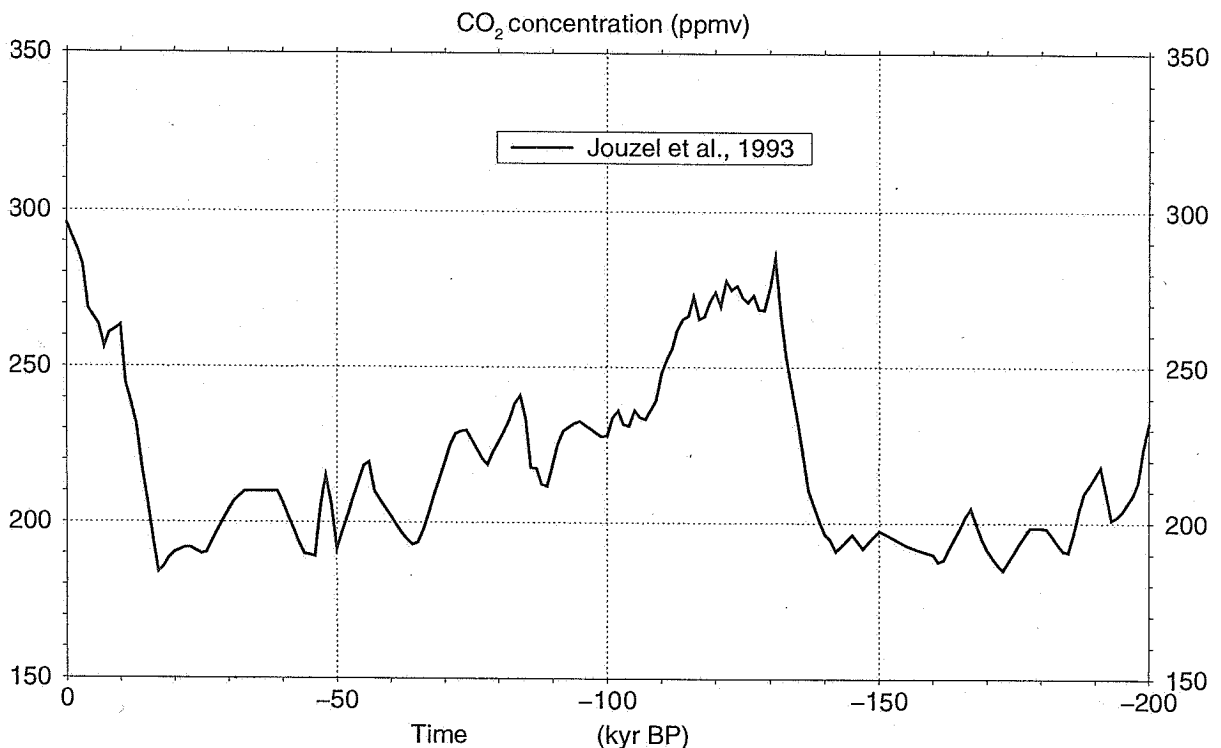


Figure 3. Atmospheric CO_2 concentration from 200 kyr BP to 130 kyr AP. For the past, the CO_2 concentration has been reconstructed from the Vostok ice core by Jouzel *et al.* (1993) using the new EGT time scale.

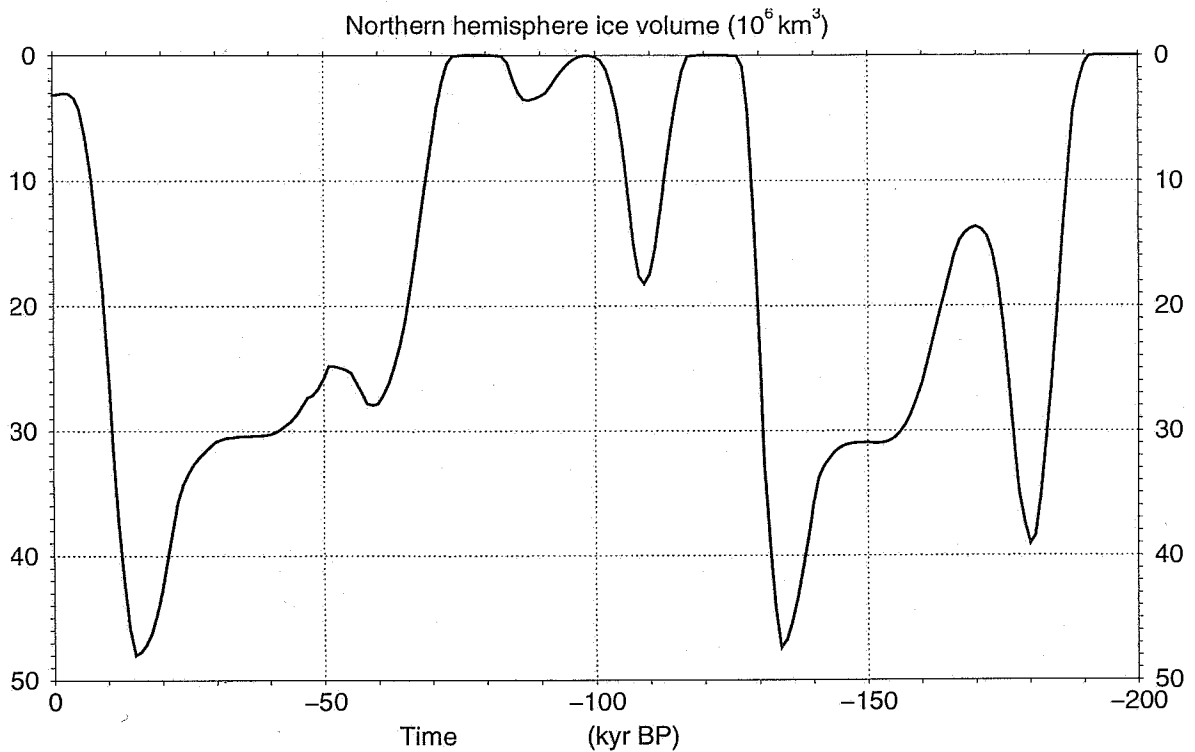


Figure 4. Simulated ice volume of the northern hemisphere using the LLN 2-D NH climate model forced by insolation and CO₂ (Berger & Loutre, 1996).

available: one based on deep-sea cores (Shackleton *et al.*, 1992) and one based on ice cores (Jouzel *et al.*, 1993, Figure 3). Sensitivity analyses have shown that the ice volumes simulated by the LLN model are very similar (almost identical) using one of these reconstructions or the other. Therefore the most direct and recent reconstruction by Jouzel *et al.* (1993) will be used in the next experiments.

Let us first remember that the peak of the penultimate interglacial is dated 215,540 yr BP (isotopic event 7.3 according to Martinson *et al.*, 1987), 200 kyr BP coinciding with isotopic event 7.2. The integration was therefore started 216 kyr BP with a Greenland ice sheet volume of $1.7 \times 10^6 \text{ km}^3$ (as it was assumed for the Eemian by Gallée *et al.*, 1992, in an earlier integration covering the last 122 kyr). At 212 kyr BP, the ice sheet has nearly completely disappeared. As we are in a decreasing phase of insolation (which occurs from 220 to 209 kyr BP at 65°N in June) this means that the size of the Greenland ice sheet assumed as initial condition at 216 kyr BP is not in equilibrium with the solar energy available in high latitudes in our model. Let us recall that our model reproduces the correct size of the Greenland ice sheet under present-day conditions, but the energy we receive now from the Sun is much lower

than at 220 kyr BP (13% lower at 65°N in June). From 212 to 203 kyr BP, the simulated ice volume is increasing again in the northern hemisphere to reach a maximum of $13 \times 10^6 \text{ km}^3$ in the middle of the increasing phase of insolation. Melting of the ice sheets is then starting and is complete at 196 kyr BP, 3000 years later than the peak of the 65°N insolation in June. If we start the integration at 200 kyr BP with a Greenland ice sheet volume of 1.7 or $3.2 \times 10^6 \text{ km}^3$, it has been shown (Berger and Loutre, 1996) that this ice sheet disappears rapidly and does not form again before 190 kyr BP. All these results confirm therefore the credibility of the initial condition used by Gallée *et al.* (1993) who started their integration at 200 kyr BP with no Greenland ice sheet, an hypothesis that we will adopt for our calculations.

Using the insolation and the Jouzel CO₂ forcings and starting our integration 200 kyr BP with no northern hemisphere ice sheets, the northern hemisphere ice volume starts to grow only after 10 kyr (Figure 4). It reaches a first maximum of $39 \times 10^6 \text{ km}^3$ at 180 kyr BP followed by a partial deglaciation leading to a minimum of $14 \times 10^6 \text{ km}^3$ of ice at 170 kyr BP. Actually the Greenland ice sheet reaches its maximum size at ~ 170 kyr BP, but the northern American and the Eura-

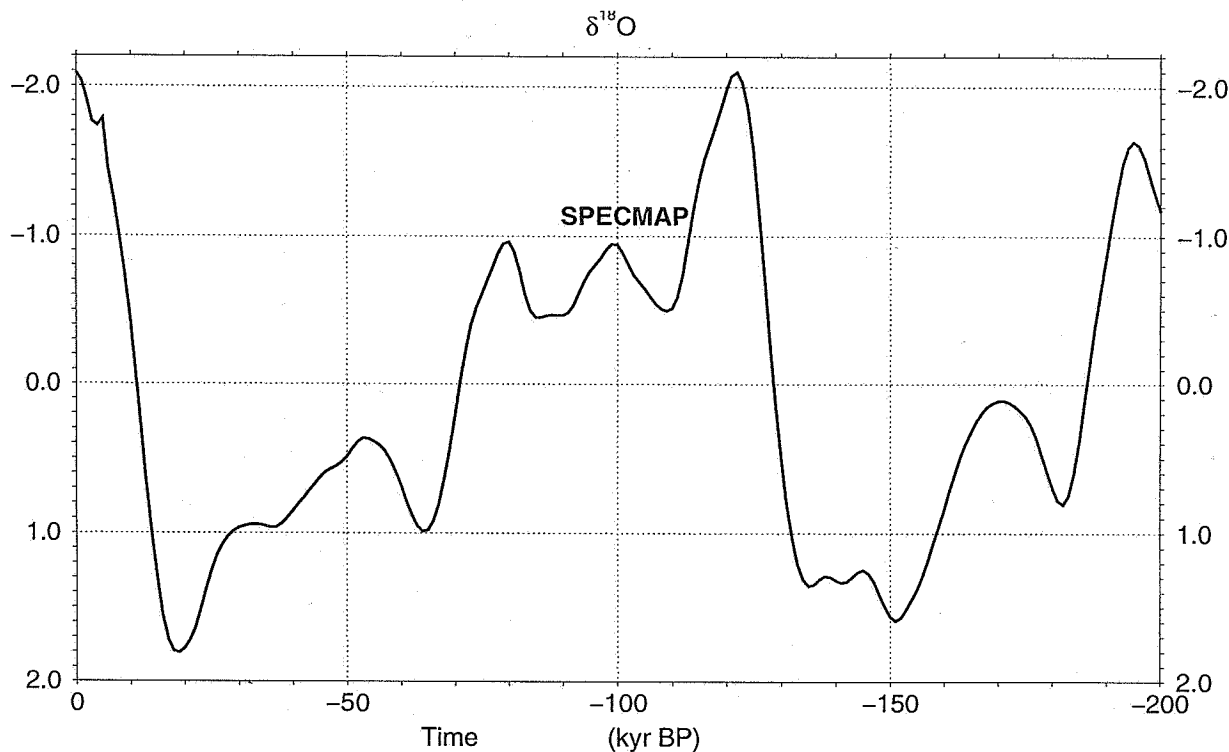


Figure 5. The stacked, smoothed oxygen-isotope SPECMAP record over the last 200 kyr (Imbrie et al., 1984; Martinson *et al.*, 1987).

sian ice sheets reach their minimum size and start to increase again up to the penultimate glacial maximum of 133 kyr BP. At this maximum, the northern hemisphere ice volume amounts to $47 \times 10^6 \text{ km}^3$, just about the same as at the Last Glacial Maximum. All the northern hemisphere ice sheets start to melt and totally disappear at 126 kyr BP, what is unrealistic according to GRIP (1993) which shows that the Greenland ice sheet has survived during the last interglacial.

It is interesting to note that the northern hemisphere ice sheets are melting totally three times in the LLN experiments: between 126 and 117 kyr BP, 100 and 97 kyr BP and 83 and 74 kyr BP. Although this is not realistic (see SPECMAP record in Figure 5), it can be explained by the large insolation occurring at these times and the large CO_2 concentration between 130 and 115 kyr BP which continues to play an important role in the behaviour of the ice sheets over the next 30 to 40 kyr.

At 70 kyr BP, the ice sheets start to form quite rapidly to lead to a first ice volume maximum at 59 kyr BP. This is followed by a weak melting of $\sim 5 \times 10^6 \text{ km}^3$ leading to a minimum in the simulated ice volume at 50 kyr BP. The ice sheets are then starting to grow again, slowly to about 30 kyr BP and then more rap-

idly to the Last Glacial Maximum where they amount to $47 \times 10^6 \text{ km}^3$ of ice at 15 kyr BP. Finally, the model simulates a deglaciation from 15 kyr to 3 kyr BP leaving only the Greenland ice sheet in the northern hemisphere with roughly $3 \times 10^6 \text{ km}^3$ of ice. Since 3 kyr BP, the ice volume is shown to increase slightly reaching $3.2 \times 10^6 \text{ km}^3$ today which represents about the present value, and our model simulation is showing that the climate has slightly cooled since the peak of the Holocene. A similar observation is clearly visible, over the whole 10,000 years, in the Greenland temperature record published by Johnsen *et al.* (1995; see their Figure 2).

Finally, integration of the model in the future for different natural CO_2 scenarios shows that the atmospheric CO_2 concentration must decrease below 250 ppmv for the ice sheets to grow in the northern hemisphere over the next 50 kyr.

5. CONCLUSIONS

A series of experiments have been made with the LLN 2-D northern hemisphere climate model to test its sensitivity to both the astronomical and the CO_2 forcings.

It must be stressed that this model is based upon a series of hypotheses and contain many parameterizations. Clouds and the hydrological cycle are oversimplified and the heat transport by the middle and deep oceans are parameterized. Despite these weaknesses, the model succeeds to simulate the long-term variations of the northern hemisphere ice sheets with an acceptable confidence. When forced by both the insolation and the atmospheric CO₂ concentration reconstructed from ice and deep-sea cores, the model simulates northern hemisphere ice volumes which are broadly in agreement with geological records and, in particular, with the stacked smoothed oxygen-isotope SPECMAP record.

6. ACKNOWLEDGMENTS

This research was partly funded by the Environment Programme of the Commission of the European Union under contract EV5V-CT92-0118. M.F. Loutre is supported by the Impulse Programme « Global Change » (contract GC/10/013, Belgian State, Prime Minister's Services, Federal Office for Scientific, Technical and Cultural Affairs). This research has benefitted from computer time provided under contract IT/SC/20 with the Belgian Research Programme on information technology. Thanks to Mr. Fr. Mercier for drawing the figures and to Mrs N. Materne-Depoorter for typing the manuscript.

7. REFERENCES

BERGER, A., 1976. Long-term variations of daily and monthly insolation during the last Ice Age. *EOS*, 57/4: 254.

BERGER, A., 1977. Support for the astronomical theory of climatic change. *Nature*, 268: 44-45.

BERGER, A., 1978. Long-term variations of daily insolation and Quaternary climatic changes. *J. Atmos. Sci.*, 35/12: 2362-2367.

BERGER, A., 1979. Insolation signatures of Quaternary climatic changes. *II Nuovo Cimento*, 2C/1: 63-87.

BERGER, A., 1988. Milankovitch theory and climate. *Rev. Geophys.*, 26/4: 624-657.

BERGER, A., GALLEE, H., FICHEFET, Th., MARSIAI, I. & TRICOT, C., 1990. Testing the astronomical theory with a coupled climate-ice sheet model. *In: Geochemical Variability in the Oceans, Ice and Sediments. Palaeogr., Palaeoclimatol., Palaeoecol.*, (89-1/2), L.D. Labeyrie and C. Jeandel (Eds). *Global Planet. Change Sect.*, 3/1-2: 125-141.

BERGER, A. & LOUTRE, M.F., 1991. Insolation values for the climate of the last 10 million years. *Quatern. Sci. Rev.*, 10/4: 297-317.

BERGER, A., LOUTRE, M.F. & TRICOT, C., 1993. Insolation and Earth's orbital periods. *J. Geophys. Res.*, 98/D6: 10341-10362.

BERGER, A. & LOUTRE, M.F., 1994. Long-term variations of the astronomical seasons. *In: Topics in Atmospheric and Interstellar Physics and Chemistry*, Cl. Boutron (ed.), Les Editions de Physique, Les Ulis, France: 33-61.

BERGER, A. & LOUTRE, M.F., 1996. Sensitivity of the LLN 2-D climate model to the astronomical and CO₂ forcings (from 200 kyr BP to 130 kyr AP). *Scientific Report*, 1996/1, Institut d'Astronomie et de Géophysique G. Lemaître, Université catholique de Louvain.

GALLEE, H., VAN YPERSELE, J.P., FICHEFET, Th., TRICOT, C. & BERGER, A., 1991. Simulation of the last glacial cycle by a coupled sectorially averaged climate ice-sheet model. I. The Climate Model. *J. Geophys. Res.*, 96: 13139-13161.

GALLEE, H., VAN YPERSELE, J.P., FICHEFET, Th., MARSIAI, I., TRICOT, C. & BERGER, A. 1992. Simulation of the last glacial cycle by a coupled, sectorially averaged climate - ice-sheet model. II. Response to insolation and CO₂ variation. *J. Geophys. Res.*, 97/D14: 15713-15740.

GALLEE, H., BERGER, A. & SHACKLETON, N.J., 1993. Simulation of the climate of the last 200 kyr with the LLN 2D-model. *In: Ice in the Climate System*, R. Peltier (ed.). *NATO ASI Series I, Global Environmental Change*, Springer-Verlag, 12: 321-341.

GRIP, Greenland Ice-core Project Members, 1993. Climate instability during the last interglacial period recorded in the GRIP ice core. *Nature*, 364: 203-207.

HAYS, J.D., IMBRIE, J. & SHACKLETON, N.J., 1976. Variations in the earth's orbit: pacemaker of the ice ages. *Science*, 194: 1121-1132.

IMBRIE, J., BERGER, A., BOYLE, E.A., CLEMENS, S.C., DUFFY, A., HOWARD, W.R., KUKLA, G., KUTZBACH, J., MARTINSON, D.G., McINTYRE, A., MIX, A.C., MOLFINO, B., MORLEY, J.J., PETERSON, L.C., PISIAS, N.G., PRELL, W.L., RAYMO, M.E., SHACKLETON N.J. & TOGGWEILER, J.R., 1993. On the structure and origin of major glaciation cycles. 2. The 100,000-year cycle. *Paleoceanography*, 8/6: 699-735.

JOHNSEN, S.J., DAHL-JENSEN, D., DANSGAARD, W. & GUNDESTRUP, N., 1995. Greenland palaeotemperatures derived from GRIP bore hole temperature and ice core isotope profiles. *Tellus*, 47B/5: 624-629.

JOUZEL, J., BARKOV, N.I., BARNOLA, J.M., BENDER, M., CHAPPELLAZ, J., GENTHON, C., KOTLYAKOV, V.M., LORIUS, Cl., PETIT, J.R., RAYNAUD, D., RAISBECK, G., RITZ, C., SOWERS, T., STIVENARD, M., YIOU, F. & YIOU, P., 1993. Vostok ice cores: extending the climatic records over the penultimate glacial period. *Nature*, 364 (6436): 407-412.

LASKAR, J., JOUTEL, F. & BOUDIN, F., 1993. Orbital, precessional, and insolation quantities for the Earth from -20 Myr to +10 Myr. *Astronomy and Astrophysics*, 270: 522-533.

MARTINSON, D.G., PISIAS, N.G., HAYS, J.D., IMBRIE, J., MOORE, T.C. & SHACKLETON, N.J. 1987. Age dating and the orbital theory of the ice ages: development of a high-resolution 0 to 300,000-year chronostratigraphy. *Quat. Research*, 27/1: 1-29.

MILANKOVITCH, M.M., 1941. Kanon der Erdbe-strahlung und seine Anwendung auf des Eiszei-tenproblem. *R. Serbian Acad., Spec. Publ.* 132, *Sect. Math. Nat. Sci.*, pp. 633 (Canon of insolation and the

ice-age problem, English translation by Israel Program for Scientific Translation, Jerusalem, 1969).

MILANKOVITCH, V., 1995. Milutin Milankovic, from his autobiography with comments by his son, Vasko, and a preface by André Berger. *European Geophysical Society*, Katlenburg-Lindau, Germany, pp. 181.

SHACKLETON, N.J., LE, J., MIX, A. & HALL, M.A., 1992. Carbon isotope records from Pacific surface waters and atmospheric carbon dioxide. *Quat. Sci. Rev.*, 11: 387-400.

Manuscript received on 23.02.1996 and accepted for publication on 11.03.96.